

# A Dynamic Light Scattering Study of Hydrogels Based on Telechelic Poly(vinyl alcohol)

Paolo Barretta,<sup>†</sup> Federico Bordi,<sup>‡,§</sup> Cristina Rinaldi,<sup>†</sup> and Gaio Paradossi<sup>\*,§</sup>

Department of Chemistry, Dipartimento di Medicina Interna, University of Rome "Tor Vergata",  
Via della Ricerca Scientifica, 00133 Rome, Italy, and INFN, Unità Roma "La Sapienza"

Received: May 22, 2000; In Final Form: July 26, 2000

Chemical hydrogels based on poly(vinyl alcohol), PVA, were obtained by reacting *telechelic* PVA bearing aldehydic groups at both ends of the chain with the hydroxylic moiety of the polymer. These networks were studied by dynamic light scattering around the sol–gel transition threshold. The auto-correlation function,  $g^{(2)}(q,t)$ , displays nonergodic behavior when the system enters the gel phase. Appropriate ensemble averaging of the  $g^{(2)}(q,t)$  yields the dynamic structure factor  $f(q,t)$ . To extract from the  $f(q,t)$  the characteristic parameters of the network, we adopted a model originally proposed for colloidal gels. A correct description of the  $f(q,t)$  was obtained. The results were compared with those obtained independently on the same type of hydrogels by equilibrium swelling and compression modulus measurements. A link to macroscopic properties of the gels is also shown.

## Introduction

Polymer hydrogels are receiving increasing attention among the scientific community. The reason for such growing interest stems from the peculiarity of their physicochemical behavior, deeply bound to their properties, and potential applications.<sup>1–8</sup> One striking feature of these materials is that some hydrogels can retain up to 99% (w/w) of water into the network meshes. Although this property is well practiced in the nature, the confinement of such an amount of water in solidlike materials opens a number of possible applications for man-made devices.

Polymer networks are usually classified into two main types, physical and chemical gels,<sup>9</sup> according to the nature of the interactions responsible for the network build up: in physical gels, interactions between chains are made of noncovalent bonds (i.e., dipolar, hydrogen, electrostatic bonds), whereas in chemical gels, covalent bonds connect the chains by means of cross-linkers.

Poly(vinyl alcohol), PVA, belongs to the limited group of biocompatible synthetic polymers.<sup>10</sup> Its tendency to form physical gels by freeze–thaw cycles is well-known in the literature.<sup>11,12</sup> A high-resolution, solid-state <sup>13</sup>C nuclear magnetic resonance (NMR) study indicated the important role of inter-chain hydrogen bonding in the formation of the physical network.<sup>13</sup> Horkay<sup>14,15</sup> has shown the possibility of obtaining chemical gels of PVA by cross-linking the polymer by an acetalization reaction between the hydroxyl moiety of the PVA chains and the aldehydic groups of a cross-linker, such as glutaraldehyde. The formation of chemical hydrogels in solution can be considered as a sol–gel transition, where the sol phase containing dilute reactants (i.e., polymer chains and cross-linker molecules) converts into a gel phase as the reaction proceeds.

Biocompatibility of PVA is a major asset for its medical application in delivery systems,<sup>6</sup> and its use as a component for tissues substitutes and for implantation of "soft" devices in

humans. The possibility to obtain a stable PVA network by a cross-linking reaction that does not involve a chemically different, scarcely tolerable, or not biocompatible reactant, is therefore an important outcome.

As any vinyl polymer, PVA bears some defects in the backbone sequence. These defects are called head-to-head units and made of few 1,2-glycol units (vicinal diols) in addition to the usual 1,3-glycolic sequences. These structural features are represented in Chart 1. The presence of head-to-head sequences is mainly due to the process of termination by coupling during the synthesis of poly(vinyl acetate),<sup>9</sup> the parent polymer from which PVA is obtained by the hydrolysis of the acetate groups. The determination of the fraction of head-to-head sequences was first addressed by Flory and Leutner,<sup>16</sup> who suggested a viscosimetric method based on the selective and quantitative oxidation by NaIO<sub>4</sub>.

We have used this reaction to split the PVA chains in a controlled way. The effects of this reaction are illustrated in Chart 1: the IO<sub>4</sub><sup>−</sup> ion splits a PVA chain where a head-to-head sequence is present, forming  $N_T$  shorter PVA chains bearing an aldehydic group at each end and two chains with only one aldehydic group corresponding to the two outmost head-to-head sequences of the starting chain. The former are usually called telechelic chains<sup>17</sup> because of the presence of the aldehydic functionality at two ends of each chain. Both the number of telechelic chains,  $N_T$ , and the number average degree of polymerization,  $\langle x \rangle_{n, \text{tel}}$ , depend on the fraction of head-to-head sequences contained in the starting PVA chains according to:

$$N_T = \frac{\Delta \langle x \rangle_{n, \text{PVA}}}{H} - 1$$

$$\langle x \rangle_{n, \text{tel}} = \frac{\langle x \rangle_{n, \text{PVA}}}{N_T + 2} \quad (1)$$

where  $\langle x \rangle_{n, \text{PVA}}$  and  $\langle x \rangle_{n, \text{tel}}$  are the number average degree of polymerization of the PVA chain before oxidation and of the telechelic chains, respectively,  $H$  is the ratio between the moles

\* Corresponding author, (e-mail: paradossi@stc.uniroma2.it).

<sup>†</sup> Department of Chemistry.

<sup>‡</sup> Dipartimento di Medicina Interna.

<sup>§</sup> INFN.



(ii) Using the nonergodic theory for getting the dynamic structural factor,  $f(q,t)$ , and the model by Krall et al. developed for internal elastic modes of a fractal gel (vide infra), allowed one to bypass the determination of a cooperative diffusion coefficient as first cumulant, which is strongly dependent on the method of getting the dynamic structure factor from the time correlation function.<sup>30</sup>

For these reasons and in the light of recent literature<sup>30,33</sup> where the dynamic behavior of a set of gels of PVA chemically cross-linked with glutaraldehyde exhibited nonergodic features, we chose to treat our DLS data by the Pusey and van Megen method.

The transition between a sol phase and the corresponding gel is characterized by a dramatic change of the normalized correlation function of the scattered electric field,  $g^{(2)}(q,t)$ :

$$g_T^{(2)}(q,t) \equiv \frac{\langle I(q,0)I(q,t) \rangle_T}{\langle I(q,0) \rangle_T^2} \quad (2)$$

where  $I(q,t) = |E(q,t)|^2$  is the intensity of the fluctuating scattered electric field at a given value of the scattering vector  $q$ , with  $q = (4\pi n/\lambda)\sin \theta/2$ , and time delay  $t$ . The difference in the correlation functions of sol and gel phases arises from the presence of a time-independent contribution to the scattered field due to nonergodic behavior of the medium or to large-scale density inhomogeneities present in the gel phase. Taking into account this contribution, the scattered electric field is written as  $E(q,t) = E_F(q,t) + E_C(q)$ . In this case, the normalized correlation function becomes:

$$g_T^{(2)}(q,t) = 1 + \frac{\langle E_F(q,0)E_F^*(q,t) \rangle_T^2 + 2I_C(q)\langle E_F(q,0)E_F^*(q,t) \rangle_T}{\langle I(q,0) \rangle_T^2} \quad (3)$$

where  $I_C(q)$  represents the intensity of scattered light corresponding to the  $E_C(q)$  component of the scattered electric field and  $\langle E_F(q,0)E_F^*(q,t) \rangle_T$  represents the time average  $\langle I_F(q,t) \rangle_T$ .

Indicating with  $\langle I(q) \rangle_E$  and  $\langle I(q) \rangle_T$  the total intensity of scattered light measured for the nonergodic system by averaging over the ensemble, and over the time, respectively, the link between these quantities is given by:

$$\langle I(q) \rangle_T = \langle I(q) \rangle_E [f(q,t) - f(q,\infty)] \quad (4)$$

where  $f(q,t)$  is the so-called intermediate scattering function.

Defining the ratio  $Y$  as:

$$Y \equiv \frac{\langle I(q) \rangle_E}{\langle I(q) \rangle_T} \quad (5)$$

we can rewrite  $g_T^{(2)}(q,t)$  in the following form:

$$g_T^{(2)}(q,t) = 1 + Y^2 \{ [f(q,t)]^2 - [f(q,\infty)]^2 \} + 2Y(1-Y)[f(q,t) - f(q,\infty)] \quad (6)$$

Solving with respect to  $f(q,t)$ , we obtain the correct normalized dynamic structure factor:

$$f(q,t) = \frac{Y-1}{Y} + \frac{1}{Y} [g_T^{(2)} - \sigma_T^2]^{1/2} \quad (7)$$

where  $\sigma_T^2$  is the mean-square intensity fluctuation,  $\sigma_T^2 = [\langle I(q)^2 \rangle_T / \langle I(q) \rangle_T^2] - 1$ .

*The Model.*<sup>25,26</sup> As for any other static or dynamic factor,  $f(q,t)$  contains the dynamic and structural characteristic parameters of the network that have to be extracted by means of a suitable model.

A chemical hydrogel is a heterogeneous system even in the ideal case of regularly spaced network chains.<sup>27</sup> Because of the intrinsic complexity of these systems, to calculate the dynamical structure factor on the basis of a model that accounts for the details of the structure and of the dynamics of the network is a difficult task. However, in recent years, several models have been proposed by different groups, describing the complex structure of these gels in terms of a fractal structure made of basic units called "blobs". We adopted the model of Krall et al.<sup>25,26</sup> for fractal gel dynamics. The model describes a nonergodic system in terms of a mechanically coupled set of "blobs". Definition of this unit is rather loose, on purpose, and by no means it is related to the chemical details of the systems, such as the functionality of the cross-links. On the other hand, an assembly of blobs is a convenient way to describe a system undergoing density fluctuation.

Because of the solidlike character of the gel, translational and rotational modes are frozen and the internal dynamics of the system is discussed in terms of subunits treated as independent damped harmonic oscillators with spring constant  $k_i$  and relaxation times  $\tau_i$ . These parameters are linked by the relationship:

$$\tau_i = \frac{6\pi\eta R_i}{k_i} \quad (8)$$

Very localized motions (i.e., small  $R_i$ ) will be characterized by small relaxation times for similar  $k_i$ s. According to the equipartition of energy principle,  $k_i \langle \Delta r_i^2 \rangle = 3K_B T$ , with  $K_B T$  having the usual meaning, the time-dependent mean squared displacement can be written for a damped harmonic oscillator as follows:

$$\langle \Delta r_i^2(t) \rangle = \frac{3K_B T}{k_i} [1 - \exp(-t/\tau_i)] \quad (9)$$

The blob mean squared displacement,  $\langle \Delta r^2(t) \rangle$ , representing the collective displacement of subunits, is given by summing all the oscillator contributions up to a cluster domain. After suitable approximations for the description of the distribution of the dimensions of the clusters, integration of eq 9, yields a stretched exponential relationship:

$$\langle \Delta r^2(t) \rangle = \frac{3K_B T}{\beta k_c \ln(f)} [1 - \exp(-t/b\tau_c)^p] \quad (10)$$

valid for a range of times up to  $10 \tau_c$  ( $k_c$  is the spring constant of the oscillator representing the cluster,  $\tau_c$  is the time needed for the cluster to relax to the equilibrium position, and  $\beta$  and  $p$  are characteristic parameters of the fractal properties of the network). Numerical integration of eq 9 over the entire set of damped harmonic oscillations made by Krall et al.<sup>26</sup> showed that eq 10 is a good approximation of the computed integral for times  $< 10 \tau_c$ .

Because  $f(q,t)$  is expressed in terms of the time-dependent displacement:

$$f(q,t) = \frac{S(q,t)}{S(q,0)} = \exp \left[ -q^2 \frac{\langle \Delta r^2(t) \rangle}{6} \right] \quad (12)$$

inserting eq 10 into eq 12 we obtain the following fitting

expression

$$f(q,t) = \exp\{-(q\delta)^2[1 - \exp(t/\tau_c)^p]\} \quad (13)$$

from which it is possible to determine  $\delta^2$ ,  $\tau_c$ , and  $p$  as fitting parameters of the intermediate correlation function  $f(q,t)$ , and differing from  $\langle\Delta r^2(t)\rangle$  and  $\tau_c$  within factors of the order of one, respectively. This equation is applied to the experimental data within the time limits given for eq 10 (i.e.,  $t \ll 10\tau_c$ ).

### Experimental Section

**Materials.** Poly(vinyl alcohol) (PVA) from Sigma (St. Louis, MO) and  $\text{NaIO}_4$  (analytical grade) from Carlo Erba (Italy), were used without further purification. Degree of deacetylation of PVA was not higher than 98% as monitored by  $^{13}\text{C}$  NMR and infrared (IR) spectra. MilliQ (Millipore, USA) water was used throughout the experiments.

**Methods.** Isothermal microcalorimetric titrations for the determination of head-to-head sequences were carried out with a TAM microcalorimeter (Thermometrics, Sweden) with the titration-perfusion accessory. The measuring cell was filled with 2 mL of an aqueous solution of PVA at a concentration of  $2 \cdot 10^{-2}$  monomol/L and titrated with a solution of  $\text{NaIO}_4$  (Carlo Erba, Italy) at a concentration of  $5.7 \cdot 10^{-3}$  M (10  $\mu\text{L}$  each addition). An integral heat of oxidation of the 1,2-glycol units by periodate of  $-232$  kJ/mol was measured, which in good agreement with periodate splitting reactions of other diols in aqueous solutions.

The  $^{13}\text{C}$  NMR spectra were collected with a Bruker AM400 spectrometer (Germany) operating at 100.63 MHz, with 5% (w/v) PVA solutions in deuterated water after accumulating 25 000 scans.

The DLS setup consisted of a 5 mW He-Ne laser source with a vat cell mounted on a goniometer plate and equipped with an optical fiber connecting the photon collection optics to the photomultiplier (Hamamatsu, Japan). Correlator (BI-9000AT) and software from Brookhaven Instruments (USA) were used with an array of 400 logarithmically spaced channels for data storage and processing.

The efficiency of the apparatus at each angle was evaluated in terms of the spatial coherence factor  $\beta$  by the Siegert relation,<sup>20</sup>  $g_T^{(2)}(q, t) = 1 + |\beta f(q,t)|^2$ , measuring the  $g_T^{(2)}(q,t)$  function of a standard polystyrene latex dispersion. In all cases, the value of  $\beta$  was  $>0.9$ .

Nonlinear fitting processing of the  $f(q,t)$  was carried out with commercial software, making use of the Marquardt algorithm.

Measurement of the number average molecular weight of PVA was determined with a membrane (cutoff, 12 000 Da) osmometer Gonotech Osmomat 090 (Germany), yielding a value of 38 000 g/mol.

The cross-linking reaction is an acid-catalyzed acetalization reaction. The time scale for the sol–gel transition is a function of the polymer concentration, the solution temperature, and the proton concentration.

We standardized the procedure according to the following conditions:

to an aqueous solution of PVA (12% w/v) was added an amount of  $\text{NaIO}_4$  to reach a value of the parameter  $H$  (molar ratio of head-to-head units over  $\text{IO}_4^-$ ) equal to 1. The oxidation of the head-to-head sequences of PVA was carried out in the dark in a closed vessel at 60 °C for  $\sim 15$  min with stirring. An almost instantaneous drop in the viscosity of the solution was the evidence of the reaction advancement. This solution, containing the telechelic chains of PVA, was cooled to room

temperature in the dark, and then a known amount of concentrated aqueous HCl was added with stirring to yield a final concentration of 1 M. Following this protocol, the gel point was reached 90 min after HCl addition. Characteristic changes in the correlation curves indicated the sol–gel transition as reported in the *Results and Discussion*. In another set of measurements, all the parameters were kept the same but the amount of  $\text{NaIO}_4$  was reduced to obtain a value of 5 for  $H$ , and the catalyst (HCl) final concentration was increased to 2.0 M. In this way, the gel point was reached after  $\sim 70$  min from the time of the HCl addition. Determination of the instrumental coherence factor,  $\beta$ , for telechelic PVA solutions at a concentration of 12% (w/v) in the initial part of the acetalization reaction was difficult because the scattering power of the solutions was limited by the reduced molecular weight of the telechelic chains. Values of  $\beta$  determined on solutions of intact PVA chains at the same concentrations were coincident, within the errors, to the values found for the latex suspensions.

For each angle, ranging from 120 to 60° in steps of 10°, measurements were carried out for a period of 8 h on freshly prepared reaction mixtures. Hydrogels formed during this period of time were clear, and data collection was not jeopardized by multiple scattering effects. The correlation function buildup was obtained in  $\sim 10$  min during the sol phase existence. To get the dynamical structure factor after the gel point, measurements of  $Y$  and  $\sigma_I^2$  as well as of  $g_T^{(2)}(q,t)$  are required. The ensemble averaged total photon counts at a given  $q$ ,  $\langle I(q) \rangle_E$ , is measured by rotating the cell with a stepping motor at a constant angular speed of 10 rpm for 10 min (“brute force method”), whereas the time average  $\langle I(q) \rangle_T$  measurement is carried out by integrating the photon counts for 10 min with the cell in a fixed position. According to eq 5,  $Y$  is given by the ratio of the two averages.

The mean-squared intensity fluctuation,  $\sigma_I^2$ , was evaluated as the intercept of the linear fitting of the initial part of the normalized correlation function  $g_T^{(2)}(q,t)$  versus  $\log(t)$  plot. This procedure was cross-checked by taking the photon counts of the first channel subtracted by the content of the last channel in the time-averaged intensity fluctuation function, corresponding to the  $\langle I(q)^2 \rangle_T$  and  $\langle I(q) \rangle_T^2$ , respectively.

### Results and Discussion

For the understanding of the dynamic and static behavior of the network, a knowledge of the structural parameters determining the mesh size is important. In this context, we studied first the amount and the distribution of the head-to-head chain sequence. Flory and Leutner<sup>16</sup> described a method for the determination of  $\Delta$  based on the use of the Mark–Howink relationship,  $[\eta] = KM^a$ , for measuring the viscosimetric average molecular weight of the PVA chains before and after periodate degradation. However, this method can be biased by the assumption that large difference in the molecular weights of these species does not imply a variations of the Mark–Howink parameters  $K$  and  $a$ .

An alternative method was developed for the determination of the fraction of head-to-head sequences,  $\Delta$ , in PVA chains based on a isothermal microcalorimetric titration of the head-to-head sequences with  $\text{NaIO}_4$ . An example of the microcalorimetric titration is given in Figure 2. In this way we have determined  $\Delta$  in available commercial samples of PVA. These findings, summarized in Table 1, are in good agreement with  $^{13}\text{C}$  NMR determination based on the ratio of the peak area of the resonances corresponding to the head-to-head methine groups (see Chart 1) with respect to the total area of the methine groups. Assignment of resonances of the head-to-head methine



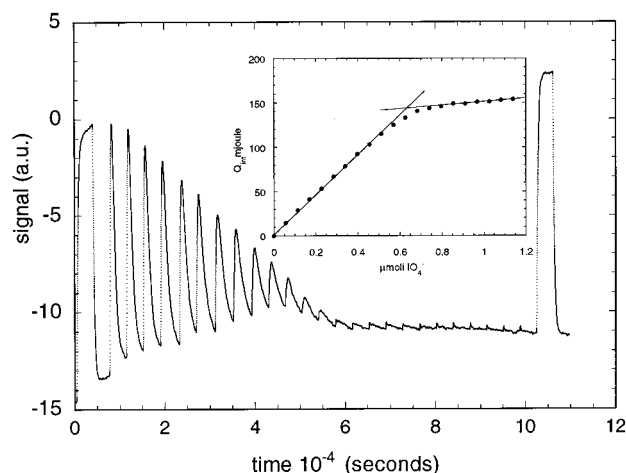


**Figure 2.** A microcalorimetric titration of the head-to-head sequence in a PVA sample. First and last peaks of the thermogram are the calibrations. Insert: Integral heat of reaction as a function of added titrant. Crossing of the lines indicates the end point of the titration. Conditions are given in the experimental part.

**TABLE 1: Fraction of Head-to-Head Sequences Determined on Different Samples of PVA**

number average molecular weight of PVA	head-to-head sequence fraction determined by:	
	titration microcalorimetry	$^{13}\text{C}$ NMR
38 000	1.5	1.3
20 000	1.1	1.2

was carried out according to previous results.<sup>36</sup> Analogous  $^{13}\text{C}$  NMR results were recently obtained by Ando.<sup>37</sup>

The threshold between the sol and gel phases was followed by DLS because this approach can detect in an unequivocal way the nonergodic behavior of the system without perturbing it in a macroscopic scale. The detection of the gel point is a well-known problem,<sup>38</sup> being related to some extent to the technique used. As pointed out by Fuchs et al.<sup>39</sup> for physical gels, rapid individuation of gel point can be achieved by following the time evolution of the amplitude and of the characteristic time of the autocorrelation function during the gelation process.

We have applied this method to the process leading to the irreversible formation of gel consisting of the chemical networking of *telechelic* PVA chains. A feature of the polymer system under study is the large difference between the intensity of the scattered light in solution and in the gel phase. This difference is due to the small size (a radius of gyration of  $\sim 27$  Å can be evaluated from the characteristic ratio and the repeating unit length of PVA, i.e., 6.4 and 1.4 Å, respectively) and low concentration of the *telechelic* PVA chains in solution. After the gel is established, a large increase of the intensity of the scattered light is measured and, as a consequence of this behavior, the dynamics of the density fluctuations was followed without the use of a dynamical probe such as latex particles<sup>34</sup> or protein molecules<sup>40</sup> dispersed in the system.

As a first step, we will consider the phenomenology of the sol–gel process followed by DLS. For the determination of the gel point we considered the experimental autocorrelation function,  $g_T^{(2)}(q, t)$ , because it is stored in the channels of the correlator both in the sol and in the gel phase. The amplitude is taken as the difference between the average value of the content of the initial five channels and of the last five channels of  $g_T^{(2)}(q, t)$ . The time corresponding to the half-height of  $g_T^{(2)}(q, t)$  is taken as a phenomenological characteristic time to be

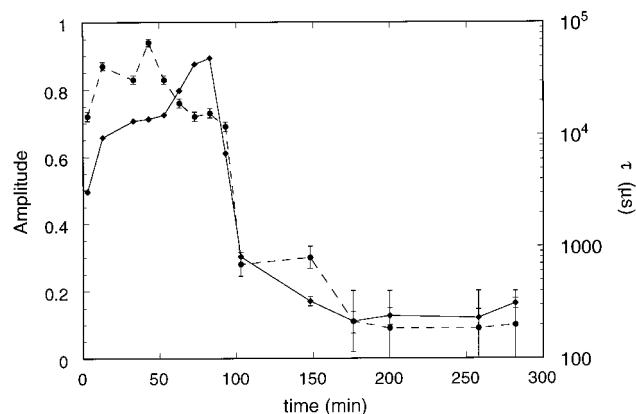


**Figure 3.** Amplitude (●) and characteristic time,  $\tau$  (◆), of the autocorrelation function  $g_2(q, t)$ .

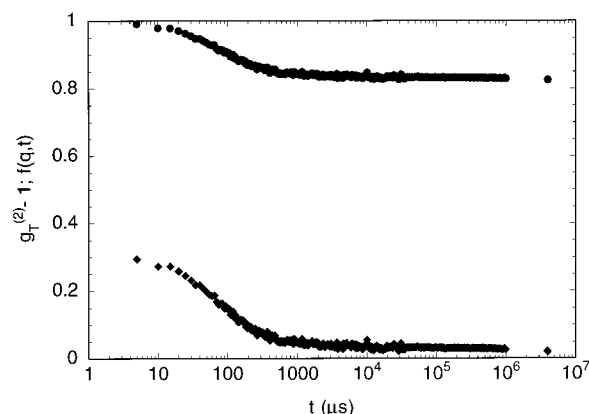


**Figure 4.** Time-averaged autocorrelation function,  $g_2(q, t)$  (◆), and ensemble averaged dynamic structure factor,  $f(q, t)$  (●), of the system in the gel phase ( $\theta = 90^\circ$ ,  $H = 5$ ).

distinguished from the correlation time values derived by the fitting procedure of the dynamic structure factor (see *Theoretical Background*) and considered in successive part of this work.

In Figure 3 we report these measured quantities as a function of the time of cross-linking reaction. Under the conditions used for this set of measurements, there is a clear drop in the amplitude values and a maximum in the characteristic time at 100 min. As predicted by the theory of DLS for nonergodic systems,<sup>22</sup> the correlation function of the scattering intensity after the threshold of the sol–gel transition undergoes a flattening due to the partially fluctuating speckle pattern characteristic of nonergodic media.<sup>27</sup> The effect of the ensemble averaging is showed in Figure 4 where the autocorrelation function  $g_T^{(2)}(q, t)$  and the dynamic factor  $f(q, t)$  are compared when the system has reached the gel state.

Tailoring the structural properties of chemically cross-linked networks is of the greatest importance for the use of these systems. The cross-linking reaction used for the synthesis of these networks allows a modulation of the average dimension of the network cages in terms of (i) length of the telechelic chains participating in the cross-linking process and of (ii) the number of the chains (see eq 1). Both these factors influence the number average molecular weight of the chain between cross-links and therefore the mesh size.

We have carried out two sets of measurements at constant chain concentration and varying the parameter  $H$  (i.e., the amount of oxidant). At chain concentration of 12% (w/v), in the first set of measurements, we used the conditions corresponding to the maximum extent of chain splitting (i.e.,  $H = 1$ ), corresponding to the smallest number average degree of

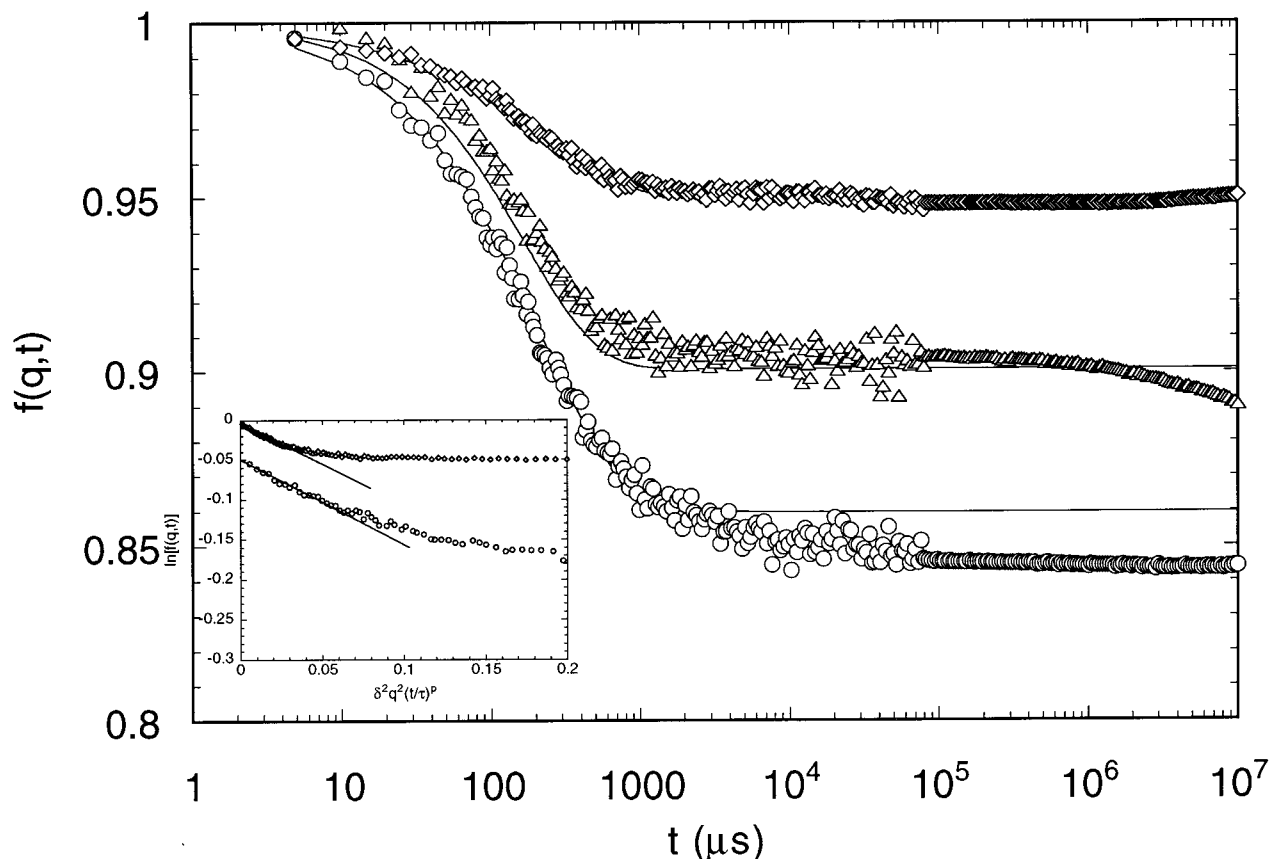


**Figure 5.** Dynamic structure factor,  $f(q,t)$ , for  $H = 1$  obtained at ( $\diamond$ )  $60^\circ$ , ( $\triangle$ )  $70^\circ$ , and ( $\circ$ )  $80^\circ$ . Full lines are the fits according to eq 13. Insert: plot of  $\ln[f(q,t)]$  as a function of the “stretched” time variable,  $\delta^2 q^2 (t/\tau_c)^p$ . Data obtained at  $80^\circ$  are shifted downward by a factor  $-0.05$ . Slopes of the linear part of the curves are 1.

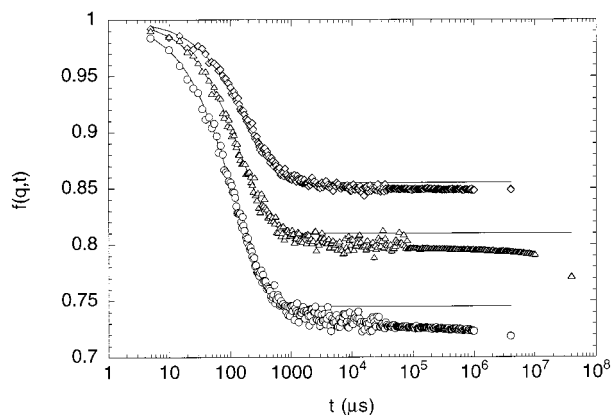


**Figure 6.** Dynamic structure factor,  $f(q,t)$ , for  $H = 5$  obtained at ( $\diamond$ )  $60^\circ$ , ( $\triangle$ )  $70^\circ$ , and ( $\circ$ )  $80^\circ$ . Full lines are the fits according to eq 13.

polymerization of the PVA chains (i.e.,  $\langle x \rangle_{n, \text{tel}} = 62$ ). In a second cycle of experiments,  $H$  was set to 5, thus yielding telechelic chains four times longer (see eq 1). Moreover, changing the chain length at constant chain concentration causes a 5-fold decrease of the terminal reactive groups concentration, resulting in a net slowing down of the cross-linking process. To obtain the formation of the gel phase approximately within the same time interval for both sets of measurements, in the samples prepared at  $H = 5$  we increased the catalyst concentration as indicated in the *Experimental Section*. In this way, we increased only the kinetics of the gel formation

In Figures 5 and 6, the ensemble averaged dynamic structure factor  $f(q,t)$  obtained according to eq 13 is showed for  $60^\circ$ ,  $70^\circ$ , and  $80^\circ$  for  $H = 1$  and for  $H = 5$ , corresponding to number average degrees of polymerization,  $\langle x \rangle_{n, \text{tel}}$ , of 62 and 240,

respectively. It is clearly shown in these figures that for both sets of measurements, the dynamic structure factor develops a nondecaying component (i.e.,  $f(q, \infty) \neq 0$ ). We interpret this behavior as an evidence for “frozen-in” motions in systems entered in a gel phase corresponding to large-scale heterogeneities.<sup>27</sup> Comparison between the  $f(q, \infty)$  values of the two gels at a given angle shows that when passing from shorter ( $H = 1$ ,  $\langle x \rangle_{n, \text{tel}} = 62$ ) to longer ( $H = 5$ ,  $\langle x \rangle_{n, \text{tel}} = 240$ ) chains, an increase of the ergodic behavior is measured. The nonergodicity of these gels is also evidenced, for a given value of chain length, by changing the value of the scattering vector,  $q$ .

Because DLS probes the dynamics of gel domains with a length scale of the order of  $q^{-1}$ , measuring the mean square displacement  $\langle \Delta r^2(t) \rangle$ , in a gel with very small mesh size, the maximum excursion will be  $< q^{-1}$  and the nonergodic behavior will be enhanced. For gels with larger mesh size, the maximum excursion will be larger and, consequently, the nonergodic features monitored by the correlation function will be less evident.

It has to be pointed out that for a fixed  $H$ , a new solution undergoing the cross-linking reaction was prepared each time to obtain the dynamic structure factor at a given angle. The measurements shown in Figures 5 and 6 have independent histories and, therefore, the time evolution of the gel phase is somewhat difficult to control because the gelation time can differ of some minutes in each preparation.

The curves are fitted according to the model proposed by Krall et al.,<sup>26,27</sup> treating the network systems as a fractal assembly of clusters composed of elements (i.e., blobs) of characteristic average dimension of  $q^{-1}$ , corresponding in our case to  $\sim 50$  nm. The fitting procedure was carried out by

**TABLE 2: Average Size of Network Meshes Determined as Adjustable Parameter  $\delta$  of the Fitting Equation 13 at Different Scattering Angles<sup>a</sup>**

$\langle x \rangle_{n, \text{tel}} = 240$		$\langle x \rangle_{n, \text{tel}} = 62$	
scattering angle, °	$\delta$ (Å)	scattering angle, °	$\delta$ (Å)
80°	340	80°	258
70°	340	70°	249
60°	336	60°	235

<sup>a</sup> Experimental errors of  $\delta$  are within  $\pm 10\%$ .

assigning decreasing weight to the plateau part of  $f(q, t)$  and using the three parameters fitting equation, eq 13, leaving  $p$  as an adjustable parameter for each measurements. The obtained values of  $p$  ranged around 0.8 and did not show any trend, being randomly fluctuating within  $\pm 10\%$ . A second-fit cycle was carried out fixing  $p$  to the mean value.

As pointed out in the original papers,<sup>26,27</sup> the model accounts for the first part of the  $f(q, t)$  time dependence, whereas experimentally, a slower process overlaps with the one considered by the model in analogy to what is usually reported for systems performing a glass transition.<sup>27</sup>

A consideration concerning the issue of the independence of the fitting parameters  $\delta$  and  $\tau$  from  $q$  for our systems is in order. We point out that for small delay times, eq 13 reduces to

$$f(q, t) = \exp(-D_p q^2 t^p) \quad (14)$$

where we have replaced the ratio  $\delta^2/\tau_c^p$  with  $D_p$ , a “stretched” diffusion coefficient. In the time range where eq 14 holds, a plot of the measured  $\ln[f(q, t)]$  as a function of  $\delta^2 q^2/(t/\tau_c)^p$  for different  $q$  values should yield decreasing straight lines with slopes equal to 1, as it is shown in the insert of Figure 5. Our systems display the linear behavior only for the initial range of delay times because of the short correlation times,  $\tau_c$ , and average displacements,  $\delta$ , measured.

The parameters  $\delta$  and  $\tau_c$  obtained from the fits account for the average dimension and for the dynamic behavior of an assembly coupled clusters.

In Figure 6, a typical trend of  $\delta$  as a function of time after gelation is shown. As expected, the process is characterized by a negative slope, indicating smaller average dimension of the network meshes as the cross-linking process builds up. This trend is linear at any of the investigated angles within the range of time studied and, within the errors, it has the same slope at any angle. This behavior is found also for  $H = 5$  (not shown).

The extrapolations of the linear trend at a zero time, represent values of the average mesh size of network when the systems begin to percolate.

The characteristic lengths obtained for PVA hydrogels with  $H = 5$  and  $H = 1$  by DLS reflect the linear dimension of the meshes of these networks and are in agreement with similar PVA networks previously studied in our laboratory<sup>18,19</sup> by compression modulus and equilibrium swelling measurements.<sup>40,41</sup> However, a strict analogy with the figures obtained in our previous work cannot be made because the preparation of gels greatly differs from that one used in this study. In fact, gels used for swelling measurements are time-invariant systems, because they have reached the final degree of cross-linking and the maximum allowed degree of swelling as the gels were sitting in water baths. In Table 2 the values of  $\delta$  extrapolated to zero time are reported.

In the stage of choosing the appropriate interpretative frame for the evaluation of the DLS results, we obtained the heterodyned correlation function corrected for the instrumental

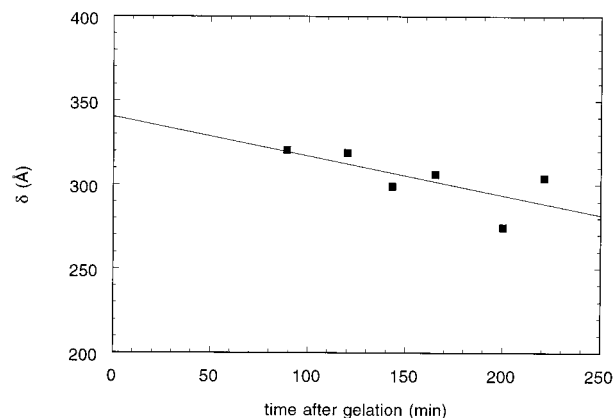


**Figure 7.** Parameter  $\delta$  (eq 13) for the indicated values for  $H = 5$  at different angles, 70° (■), as a function of the time after gelation.

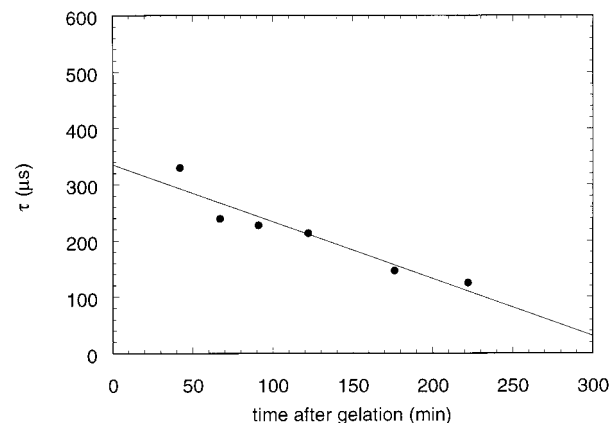


**Figure 8.** Typical time evolution of  $\tau$  for  $H = 1$ ,  $\theta = 80^\circ$ .

coherence factor from the time intensity correlation function,  $g_T^{(2)}(q, t)$ , as suggested by Geissler.<sup>30,32</sup> In this way, we obtained a cooperative diffusion coefficient,  $D_c$ , and an average polymer chain distance,  $\xi$ , as first cumulant of the heterodyned correlation function and by means of the Stokes–Einstein relationship  $\xi = kT/6\pi\eta_0 D_c$ , respectively. Values of  $\xi$  obtained by this method for hydrogels prepared by using telechelic PVA with different chain length showed a mismatch between the parameter  $\xi$  and the length of the PVA telechelic chain used in the cross-linking process.

This finding cannot be considered to hold in general. As already pointed out in the paper of Fang et al.,<sup>30</sup> gels differing in the chemical structure and architecture of the polymer network have different DLS behaviors. Therefore, an analysis of the observed correlation functions by the available methods and comparative studies of the parameters obtained by DLS and other independent approaches has to be carried out for a given system.

The behavior of  $\tau_c$ , Figure 8, during the cross-linking reaction shows a trend toward smaller values. This trend indicates that, within the interpretative frame of Krall et al., the dynamics of the clusters becomes more restricted and/or localized.

Finally, this model allows a link between the macroscopic properties of the gels and the fitting parameters obtained from the measure of the dynamic structure factor  $f(q, t)$  because the elastic modulus,  $G$ , of the gel can be evaluated according to the relationship  $G \approx k_c/R_c$ , where the mechanical coupling of two clusters at distance  $2R_c$  is described by an elastic force with an effective spring constant  $k_c$ . Figure 9 shows the behavior of the elastic modulus on the gelation time, that is, on the increase in the cross-linking density.

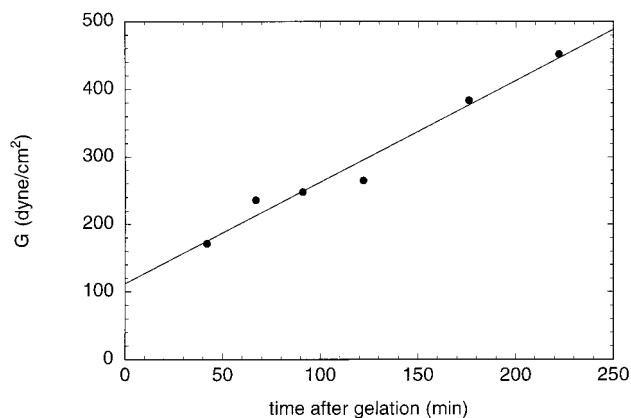


**Figure 9.** Elastic modulus as a function of gelation time for  $H = 1$  (●), measured at  $\theta = 80^\circ$ .

### Concluding Remarks

The results of the DLS study of the cross-linking reaction of telechelic PVA was evaluated with a fractal model that has to date been used for colloidal suspensions reaching a diffusion-limited colloidal aggregation limit. Despite the difference between polymeric chemical gels and colloidal gels, the dynamic and structural parameters evaluated with the aid of this model on gels of telechelic PVA is compatible with the results obtained on the same systems with macroscopic equilibrium measurements. This issue has to be examined for a wider range of polymers and gelation conditions. However, a possible factor contributing to the essentially correct description of the system under investigation by this model can be viewed in the very coarse networking of the chains that, at least in the early stages of the gelation examined in this work, has a connectivity spanning average distances of the order of magnitude of  $q^{-1}$ . The nonergodic method was used for treating DLS data considering the findings obtained on other PVA chemical hydrogels and the unsatisfactory results obtained with other available treatments of DLS data. However, general criteria on the choice of method to be adopted cannot be formulate at the present time.

### References and Notes

- (1) *Hydrogels and Biodegradable Polymers for Bioapplications*; Ottenbrite, R. M., Huang, S. J., Park, K., Eds.; American Chemical Society: Washington, DC, 1996.
- (2) *Biological and Synthetic Polymer Networks*; Kramer, O., Ed.; Elsevier: New York, 1988.
- (3) *Physical Networks, Polymers and Gels*; Burchard, W., Ross-Murphy, S. B., Eds.; Elsevier: New York, 1990.
- (4) Guenet, J. M. *Thermoreversible Gelation of Polymer and Biopolymers*; Academic Press: London, 1992.
- (5) *Physical Properties of Polymeric Gels*; Cohen Addad, J. P., Ed.; J. Wiley: New York, 1996.
- (6) *Biomedical Applications of Hydrogels: Review and Critical Appraisal*; Williams D. F., Ed.; CRC Press: Boca Raton, FL, 1981.
- (7) Kajiwar, K.; Ross-Murphy, S. B. *Nature* **1992**, *355*, 208.
- (8) Van der Zande, B. M. I.; Pagès, L.; Hikmet, R. A. M.; van Blaaderen, A. *J. Phys. Chem. B* **1999**, *103*, 5761.
- (9) Flory P. J. *Principles of Polymer Chemistry*, 14th ed.; Cornell University Press: Ithaca, NY, 1990; Chapter 13.
- (10) *Polyvinyl Alcohol: Properties and Application*, Finch, C. A., Ed.; J. Wiley: New York, 1973.
- (11) Peppas, N. A.; Scott, J. E. *J. Controlled Release* **1992**, *18*, 95.
- (12) Hassan, C. M.; Peppas, N. A. *Macromolecules* **2000**, *33*, 2472.
- (13) Kobayashi, M.; Ando, I.; Ishii, I.; Amiya, S. *Macromolecules* **1995**, *28*, 6677.
- (14) Horkay, F.; Burchard, W.; Geissler, E.; Hecht, A. *Macromolecules* **1993**, *26*, 1296.
- (15) McKenna, G.; Horkay, F. *Polymer* **1994**, *35*, 5737.
- (16) Flory, P. J.; Leutner, F. S. *J. Polym. Sci.* **1948**, *3*, 880.
- (17) Goethals, E. J. *Telechelic Polymers: Synthesis, Properties and Applications*; CRC Press: Boca Raton, FL, 1989.
- (18) Paradossi, G.; Lisi, R.; Paci, M.; Crescenzi, V. *J. Polym. Sci. Part A: Polym. Chem.* **1996**, *34*, 3417.
- (19) Paradossi, G.; Cavalieri, F.; Capitani, D.; Crescenzi, V. *J. Polym. Sci. Part B: Polym. Phys.* **1999**, *37*, 1225.
- (20) Berne, B. J.; Pecora, R. *Dynamic Light Scattering*; J. Wiley: New York, 1976.
- (21) Schmitz, K. S. *An Introduction to Dynamic Light Scattering by Macromolecules*; Academic Press: Boston, 1990.
- (22) Pusey, P. N.; van Megen, W. *Physica A* **1989**, *157*, 705.
- (23) Van Megen, W.; Pusey, P. N. *Phys. Rev. A* **1991**, *43*, 5429.
- (24) Pusey, P. N.; van Megen, W. *Phys. Rev. Lett.* **1987**, *157*, 705.
- (25) Gang, H.; Krall, A. H.; Cummins, H. Z.; Weitz, D. A. *Phys. Rev. E* **1999**, *59*, 715.
- (26) Krall, A. H.; Weitz, D. A. *Phys. Rev. Lett.* **1998**, *80*, 778.
- (27) Krall, A. H.; Huang, Z.; Weitz, D. A. *Physica A* **1997**, *235*, 19.
- (28) Shibayama M. *Macromol. Chem. Phys.* **1998**, *199*, 1.
- (29) Pütz, M.; Kremer, K.; Everaers, R. *Phys. Rev. Lett.* **2000**, *84*, 298.
- (30) Fang, L.; Brown, W. *Macromolecules* **1992**, *25*, 6897.
- (31) Fang, L.; Brown, W. *Macromolecules* **1990**, *23*, 3284.
- (32) Geissler, E. In *Dynamic Light Scattering, the Method and Some Applications*; Brown, W., Ed.; Oxford University Press: Oxford, England, 1993.
- (33) Kjøniksen, A.; Nyström, B. *Macromolecules* **1996**, *29*, 7116.
- (34) Joosten, J. G. H.; Geladé E. T. F. *Phys. Rev. A* **1990**, *42*, 2161.
- (35) Joosten, J. G. H.; McCarthy, J. L.; Pusey, P. N. *Macromolecules* **1991**, *24*, 6690.
- (36) Vercauteren, F. F.; Donners, W. A. B. *Polymer* **1986**, *27*, 993.
- (37) Ando, I.; Kobayashi, M.; Kanekiyo, M.; Kuroki, S.; Ando, S.; Matsukawa, S.; Kurosu, H.; Yasunaga, H.; Amiya, S. NMR Spectroscopy in Polymer Science. In *Experimental Methods in Polymer Science*; Tanaka, T., Ed.; Academic Press: San Diego, CA, 2000.
- (38) Ross-Murphy, S. B. *J. Rheol.* **1995**, *34*, 1451.
- (39) Fuchs, T.; Richtering, W.; Burchard, W.; Kajiwar, K.; Kitamura, S. *Polym. Gels Networks* **1997**, *5*, 541.
- (40) Sellen, D. B. *J. Polym. Sci. Part B: Polym. Phys.* **1987**, *25*, 699.
- (41) Peppas, N. A.; Merrill, E. W. *J. Polym. Sci., Polym. Chem. Ed.* **1997**, *14*, 441.
- (42) *Hydrogels in Medicine and Pharmacy*; Peppas, N. A., Ed.; CRC Press: Boca Raton, FL, 1986; Chapter 2.